



# The effect of 3, 3', 3'',3'''-tetra poly- (1, 4-phenylene terphthalamide) phthalocyanine copper(II) in intermediate layer on the performance of active layer solar cells

Abdullah Abbas. Hussein<sup>1</sup>, Adil Ali Al-Fregi<sup>2</sup> & Ziyad T. Al-Malki<sup>3</sup>

<sup>1</sup> Department of Material Science, Polymer Research Centre, University of Basrah

<sup>2</sup> Department of Chemistry, College of Science, University of Basrah

<sup>3</sup> Department of Chemistry, Polymer Research Centre, University of Basrah

E-mail: :author@univsul.net

## Article info

Original: 27 Oct. 2014  
 Revised: 27 Jan. 2015  
 Accepted: 22 Feb. 2015  
 Published online:  
 20 June 2015

## Key Words:

PEDOT: PSS, Buffer intermediate layer,  
 P3HT: PCBM,  
 Phthalocyanine,  
 grafted polymer

## Abstract

A new phthalocyanine grafted polymer namely 3, 3', 3'', 3'''-Tetra{ poly- (1, 4-phenylene isophthalamide)} phthalocyanine copper (II) (TPPT) has been prepared and characterized by IR, U.V-visible spectroscopies. 3, 3', 3'', 3'''-Tetra{ poly- (1, 4-phenylene isophthalamide)} phthalocyanine copper (II) (TPPT) deposited at the interface of the hole collecting buffer intermediate layer [poly(3,4ethylenedioxythiophene): poly(styrene sulfonate) (PEDOT: PSS)] and poly (3-hexylthiophene): [6,6]-phenylC61 butyricacidmethylester (P3HT:PCBM) active layer were found to significantly increase solar cell performance. The "photo-physical" properties of these devices incorporated with (TPPT) with different space distributions at the interface of PEDOT: PSS buffer intermediate layer, and P3HT: PCBM active layer were investigated. We find that, the optical property was improved as the TPPT are large enough to penetrate into the active layer and the performance of organic solar cells (OSCs) with large TPPT can benefit from the improved hole collection efficiency. The power conversion efficiency (PCE) enhancement for the device with a PEDOT: PSS. TPPT film is more significant than for the device with PEDOT: PSS film. PSCs give Power Conversion Efficiency (PCE) of 0.14%, for ITO/PEDOT:PSS: TPPT/P3HT: PCBM/Al devices.

## I. INTRODUCTION

Phthalocyanines are solid materials also known as aza porphyrin derivatives. They are the class of synthetic tetrapyrrolic compounds which are structurally similar to the naturally occurring porphyrin [1,2], such as hemoglobin, chlorophyll and vitamin B12 but phthalocyanines themselves do not occur in nature[1,2].

The phthalocyanines are planar aromatic macrocycles and consisting of four isoindole subunits presenting an 18-electron aromatic cloud delocalized over an arrangement of alternated carbon and nitrogen atoms [1,2]

Barett *et. al.* showed that the phthalocyanine is a macrocyclic material composed of four isoindole units with a central cavity of sufficient size to accommodate various metal ions [1,2].

Phthalocyanine and its derivatives constitute one of the most studied classes of organic functional materials in nonlinear optics, liquid-crystalline electronic charge carriers, exciton-transport materials, optical data storage, photodynamic cancer therapy.

The central cavity of phthalocyanines can be complex with 63 different elemental ions in periodic table by replacing the two central hydrogens atoms, phthalocyanine containing one or two metal ions is called a metal phthalocyanine (Mpc) [1,2]. Syntheses of phthalocyanines from phthalonitrile or phthalic anhydride in the presence of urea are the most two important laboratory and industrial methods which were used. Originally by Linstead and coworkers [3]. The nitration of phthalocyanines is impossible because of the high stability, so that nitro phthalocyanines was prepared from nitro phthalic acid or nitro phthalic anhydride [4]. Nitro phthalocyanines were reduced to amino phthalocyanines by using certain reducing agent mainly, Na<sub>2</sub>S·9H<sub>2</sub>O [5]. Grafting phthalocyanine amino derivatives with different prepared polymers having carboxyl end groups can be prepared by simple condensation reaction [6].

On the other hand, the effective conversion of solar energy into electricity is becoming a very important issue for past few years in terms of rising energy costs and needs. Polymer Photovoltaic cells offer a great technological potential as renewable energy sources for electrical energy and offer easily manufactured, compatibility with flexible substrates and low-cost alternative to the traditional inorganic-based solar cells [7–12]. Various strategies were worked in the fabrication of efficient polymer photovoltaic cells. In the past, bulk heterojunction photovoltaic cells (BHJ) made by blending p-type p-conjugated polymer with n-type fullerene materials were studied extensively [13].

To significantly enhance the photovoltaic efficiency is still one of the most important tasks for the polymer photovoltaic cells. The light to electricity conversion process involves four steps: (1) light absorption and exciton formation, (2) exciton dissociation, (3) charge transport, and (4) charge collection. These four steps are affected by the chemical structure of active materials, that is, the donor and the acceptor and the morphology of the active polymer film [11–16]. P3HT polymer and PCBM fullerene become popular donor and organic acceptor for polymer photovoltaic cells due to their easy availability, excellent solubility in common organic solvents, and high mobility. Recently, great progress was made on P3HT:PCBM photovoltaic cells.

poly(3-hexylthiophene) absorbs a part of the visible light (vis-light), which limits the interest of sunlight. This aside, the "high lying" highest occupied molecular orbital HOMO energy level in P3HT also limits the open circuit voltage ( $V_{oc}$ ), resulting in a low PCE [16]. The  $V_{oc}$  of a PSC was closely related to the energy offset between the HOMO of the donor and the LUMO of the acceptor [12]. Until now, a lot effort has been devoted to developing new solution processable donor materials with low lying highest occupied molecular orbital levels, and establishing what their properties should offer efficient OSCs by mixing with fullerene PCBM.

Phthalocyaninato based materials have shown very promising properties for application in PSCs, due to their relatively large and planar conjugated structure that are favorable to facial p–p stacking, thus benefiting charge transportation and the absorption of long wavelengths [17–20]. A series of copper (II) phthalocyanine containing low band gap copolymers were used in OSCs [9]. Because its rigid, higher mobility and planar structure, the incorporation of a low bandgap unit into the phthalocyanine copper (II) unit could potentially result in a red-shift in absorption. A more appropriate energy level was obtained by fine tuning the molecular structure for photovoltaic application.

In this research, we have studied the effect of additive TPPT on the performance, crystallinity and the interface morphology of ITO/PEDOT:PSS /P3HT:PCBM/Al devices.

## II. EXPERIMENTAL

### A. Material

Regioregular – poly (3-hexylthiophene) P3HT , [6,6]-phenyl C61-butyricacidmethylester PCBM, [poly (3,4ethylenedioxythiophene): poly (styrene- sulfonate) (PEDOT:PSS)] (Sigma-Aldrich- as received), acetone, isopropyl alcohol , chloro- benzene , 1,4- diaminobenzene,dimethylformamide DMF, phthalic anhydride, sulfuric acid, nitric acid, acetic anhydride, ammonium molybdatetetra- hydride , hydrochloric acid, sodium hydroxide, sodium sulfide nonahydrate, terphthalic acid, and thionylchloride were purchased from Aldrich Chemical Company.

### B. Synthesis

#### Preparation of 3-nitro phthalic acid [21]

3-nitrophthalic acids was prepared by nitration of phthalic anhydride as the following procedure:- Phthalic anhydride (50g, 5 moles) was dissolved in 50ml of conc. sulfuric acid at 75°C, and then 21 ml of fuming nitric acid was added with vigorous stirring at 90°C. 15 ml of sulfuric acid was added dropwise for 1 hr, next 90 ml of nitric acid was added at 90°C with vigorous stirring for 3 hours .After cooling, the mixture was filtered to remove the excess of nitric acid and sulfuric acid. The crude product washed several times with distilled water. Pale yellow powder was obtained m.p 218°C (lit. 218°C), yield 40%.

#### Preparation of 3-nitro phthalic anhydride [17]

3- nitrophthalic acid (0.1 mole) was added to acetic anhydride (20 g, 0.19 mole ) and the mixture was refluxed for 1 hr . After cooling, the mixture was filtered and the solid product washed several times with absolute ethanol followed by filtration and dried in air for a short time, m.p. 163°C (lit. 163°C) yield 90%.

#### Preparation of 3, 3', 3",3'''-tetra nitro phthalocyaninatocopper (II) (NO<sub>2</sub>)<sub>4</sub>PcCu(II) [18]

CuCl<sub>2</sub> (0.50 g , 8 mmole) , 3-nitrophthalic phthalic anhydride (4.73 g , 32 mmole) , ammonium molybdate tetrahydride (0.2 g) ammonium chloride (0.5 g, 9 mmole) and excess of urea (30g , 0.5 mole) were grounded and placed in 250 ml round bottom flask containing 100 ml of nitrobenzene . The temperature of the stirred reaction mixture was gradually increased to 185°C and maintained it for 5 hr. The hot mixture was filtered and the precipitate washed with ethanol repeatedly to remove the nitrobenzene. The solid product was dried and added to 200 ml of 1 N HCl and then refluxed for 1 hr, cooled to room temperature and filtered. The solid precipitate added to 200 ml of 1 N NaOH and reflux the solution for 1 hr, filtered and washing with distilled water to obtain blue crystals of 3, 3', 3",3'''-nitrophthalocyaninato copper(II) ; yield 85%.

#### Preparation of 3, 3', 3",3'''-tetra amino phthalocyaninato copper(II) (NH<sub>2</sub>)<sub>4</sub>PcCu(II) [22]

A mixture of 3, 3', 3",3'''-tetra nitro phthalocyaninato copper(II) (4 g, 0.0053 mol) and (10 g, 0.041 mol) of sodium sulfide nonahydrate in 50 mL of distilled water was heated at 60°C with stirrer for 12 hr. The reaction mixture was cooled and filtered. The solid product was refluxed with 50 mL of aqueous solution of 0.5N of sodium hydroxide for 1hr., followed by aqueous solution of 0.5N of hydrochloric acid for 1hr. The mixture was filtered and washed with hot water and dried at 110 °C. The final blue powder product 3, 3', 3",3'''-tetra amino phthalocyaninato copper(II) was formed, yield 70%.

#### Preparation of Poly(1,4-phenylene terphthal amide) (PPT) [23]

Poly(1,4-phenylene terphthal amide) was prepared by simple condensation polymerization of 1,4-diaminobenzene(10.81g, 0.1 mol) was dissolved in dry dichloromethane (100 mL), and the solvent was distilled to a final volume of 50 mL to remove the residual water. Terphthaloyl chloride (20.30 g, 0.1 mol) and triethyl amine (20. 2 mL, 0.2 mol) were added to the reaction mixture, and stirred at room temperature over night. The product was precipitated by slowly addition to diethyl ether. The resulting polymer was obtained as white solid which was collected by filtration and drying, yield 90%.

**Prepaation 3, 3', 3'', 3'''-Tetra { poly- (1, 4-phenylene terphthalamide)} pthalocyaninato copper (II) (TPPT) [24]**

3, 3', 3'', 3'''-tetraamino pthalocyaninato copper(II) ( 7.67 g , 10 mmole) was suspended in 50 mL of toluene and was added to polmer solution of poly(1,4-phenylene terphthalamide)( 5 g) in 50 mL of toluene. The mixture was refluxed for 5hr and left to cool down to ambient temperature. The solid product was dried at room temperature, yield 78%.

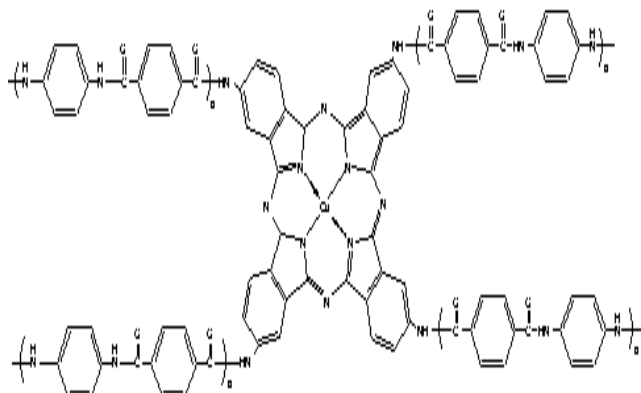
**Photovoltaic Device Fabrication**

Each glass substrate was coated with a transparent ITO electrode (120 nm thick,  $15\Omega/\text{sq}$  sheet resistance), washed thoroughly in acetone, isopropyl alcohol, and distilled water, dried under nitrogen gas, heat dried, and finally treated by ozone–ultraviolet cleaner for10min. The prepared PEDOT:PSS (Sigma-Aldrich) solution was mixed with

3, 3', 3'', 3'''-Tetra{ poly- (1, 4-phenylene terphthalamide)} pthalocyaninato copper (II)(TPPT). The concentration of TPPT in PEDOT:PSS 0.2 wt.%. Then this solution was spin coated at 2500rpm on onto ITO substrate (20nm) which was pre-coated on the surface of the active layer. Thermal pre-annealing was conducted at  $150^{\circ}\text{C}$  for 15min on a dry oven in ambient air. The mixed solutions consisting of rr-P3HT,(10 mg  $\text{mL}^{-1}$ ) and PCBM ( $10\text{mgmL}^{-1}$ ) in solvent chlorobenzene (CB) solvent was then spin-coated at 1000 rpm on the PEDOT:PSS layer in air. The thickness of the active layer is  $\sim 150$  nm. After spin-coating photoactive layer, Al (40nm) was thermal evaporated under high vacuum of  $\sim 2\times 10^{-5}\text{Pa}$  with a rate of  $0.1\text{ nm s}^{-1}$  onto the polymer layer as a cathode to create a device with an active area of  $9\text{mm}^2$  defined by a shadow mask. The final device structure is ITO/PEDOT:PSS TPPT/P3HT: PCBM/Al, as shown in Fig.1(a&b). Finally the post-annealing of the completed photovoltaic cells was carried out at  $120^{\circ}\text{C}$  for 20 min inside the glove box.

**III. Device Characterization**

The current density–voltage (J–V) characteristics of devices were measured with a computer-programmed Keithley 2400 source/meter, which simulated the AM1.5 sunlight with energy density of  $100\text{mWcm}^{-2}$ . Films were prepared by spin coating PEDOT:PSS (TPPT) and P3HT: PCBM solution on glass substrates for UV–vis absorption spectroscopy and atomic force microscopy (AFM). The UV–vis absorption spectra of the polymer films were taken with a Varian Cary 5000UV–VIS–NIR spectrometer. The light intensity for the solar simulator was calibrated with a standard photovoltaic (PV) reference cell. Incident photon to electron conversion efficiency (IPCE) curves were measured with a Stanford lock-in amplifier 8300 unit.The AFM images of the polymer films were acquired using a BRUKER NanoScope IV Multi-Mode Adapter AFM with the tapping mode. The film thickness was measured by spectroscopic ellipsometry (M-2000).



a

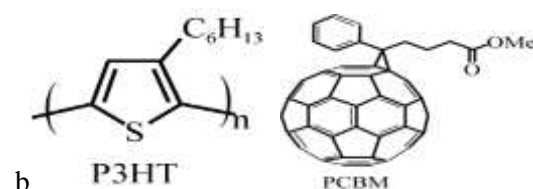


Fig.1 Chemical structure of (a) TPPT (b) PH3T and PCBM.

#### IV. Results and Discussion

3- nitrophthalic anhydride was prepared in situ from nitration of phthalic anhydride by  $\text{HNO}_3$  and  $\text{H}_2\text{SO}_4$  . The catalyst ammonium molybdate tetrahydrate is very important in preparative method in increasing the yields of complexes, reducing reaction time and decreasing the reaction temperature.  $(\text{NO}_2)_4\text{PcCu}(\text{II})$  was prepared by using 3-nitrophthalic acid but cannot by direct nitration of phthalocyanine copper (II) because these complexes have higher stability against these reagents.  $(\text{NO}_2)_4\text{PcCu}(\text{II})$  was converted to  $(\text{NH}_2)_4\text{PcCu}(\text{II})$  by reacting it with sodium sulfide nonahydrate *i.e* reduction the nitro groups to amine groups. All prepared compounds cannot be purified by recrystallization method because has no solubility in most organic and inorganic solvents . The purification of the prepared compounds was carried out by dissolving in HCl then with NaOH. Generally, the prepared complexes are insoluble in water and ethanol and not sensitive to hydrolysis but can be dissolved in DMSO , DMF. The prepared compounds were decomposed up to  $300^{\circ}\text{C}$ . The high thermo – stability of prepared compounds can be attributed to the aromatic system of phthalocyanine molecule with highly resonance structure. The copper (II) ion fitting with space inside phthalocyanine molecule also enhance this thermal stability.

Because of the limited solubility of all the prepared compounds in most common organic solvents, therefore, they are characterized by IR spectroscopy in form of KBr disc. The IR data of all compounds display characteristic bands at certain frequencies. The observed vibration bands are similar to these in the literature and typical representative of IR spectra for metallo phthalocyanines complexes.

The IR spectra of IR spectrum of  $(NO_2)_4PcCu(II)$ , Fig. 2 shows two stretching bands, the first band at  $1537\text{cm}^{-1}$  due to a symmetrical stretching of  $NO_2$  groups, while the other can be assigned to symmetrical stretching of  $NO_2$  groups at  $1342\text{cm}^{-1}$  [24, 25]. The main features of reduction of nitro groups in  $(NO_2)_4PcCu(II)$  to amino groups in  $(NH_2)_4PcCu(II)$  is disappear of the bands which assigned for nitro group bands and appear two new bands at  $3431$  and  $3338\text{cm}^{-1}$  which can assigned for asymmetric and symmetric stretching bands of  $NH_2$  groups, while the bending band of  $N-H$  appeared in  $1622\text{cm}^{-1}$  [24, 25], Fig. 3. Both spectra of compounds  $(NO_2)_4PcCu(II)$  and  $(NH_2)_4PcCu(II)$  show a weak band can be due to  $Cu-N$  stretching at  $538$  and  $545\text{cm}^{-1}$  [26] this indicate that all the prepared complexes in cis form adopting  $D_{4h}$

point group .The IR spectra , Fig. 2 and 3 show a strong bands in the range 1483-1400  $\text{cm}^{-1}$  and 1340- 1313  $\text{cm}^{-1}$  due to asymmetrical and symmetrical stretching C=C[24, 25]. Also, both spectra of  $(\text{NO}_2)_4\text{PcCu(II)}$  and  $(\text{NH}_2)_4\text{PcCu(II)}$  show several bands ranged 1150-700  $\text{cm}^{-1}$  assigned to the phthalocyanine skeletal vibrations[27]. The aromatic C-H stretching bands appear in range 3015-3035  $\text{cm}^{-1}$  while the stretching band of C-N bond at 1249and 1269  $\text{cm}^{-1}$ , respectively[24, 25].

The IR spectrum of the prepared polymer, *i.e.* poly- (1, 4-phenylene terphthalamide) (PPT), Fig. 4 and grafted phthalocyanine copper (II), *i.e.* 3, 3', 3'', 3'''-tetra{ poly- (1, 4-phenylene terphthalamide)} phthalocyaninato copper (II) (TPPT), Fig. 5, show a broad band of N-H stretching of amide groups at 3335 and 3350  $\text{cm}^{-1}$  respectively while the N-H bending vibration at 1580 and 1520respectively[24, 25]. . Stretching band of C=O of amide groups in both (PPT) and (TPPT) compounds appear at 1694 and 1704  $\text{cm}^{-1}$  respectively[24, 25]. The aromatic C-H stretching bands of (PPT) and (TPPT) appear at 3042-3026  $\text{cm}^{-1}$  while the stretching band of C-N bond at 1280 and 1269  $\text{cm}^{-1}$ , respectively[24, 25].

The U.V-visible data of all prepared complexes recorded in the range 200-800 nm using DMF as solvent, Figs. 6-8.

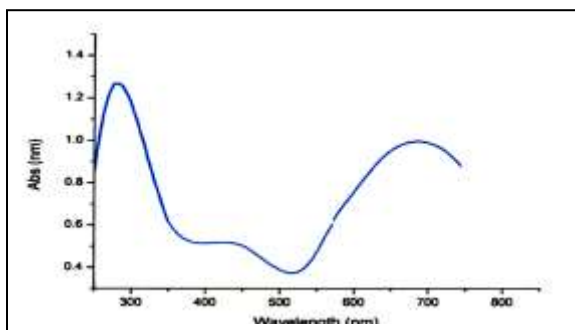


Fig. 6 : Uv-vis spectrum of 3,3',3'',3'''-( $\text{NO}_2$ )<sub>4</sub>PcCu(II)

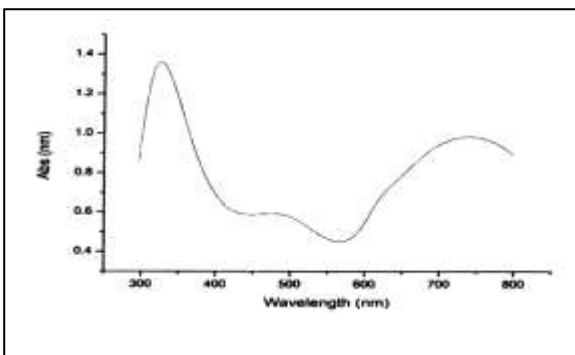


Fig. 7 : Uv-vis spectrum of 3,3',3'',3'''-( $\text{NH}_2$ )<sub>4</sub>PcCu(II)

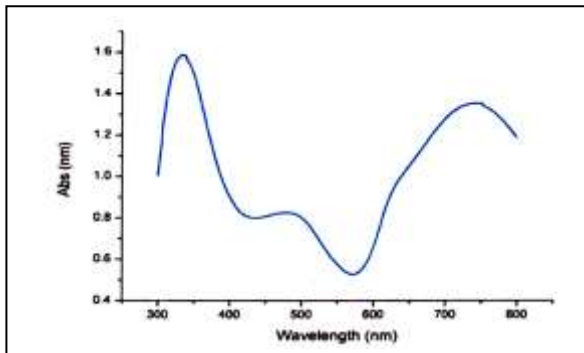


Fig 8 : Uv-vis spectrum TPPT

There is considerable interest in the characterization of the electronic structure of phthalocyanines. The main and most characteristic feature of the absorption spectra of phthalocyanines is the presence of two very

intensive bands, one in the visible region called the Q-band and the second band in the UV region called B- or the soret band, which is related to the valence bond structure[27-29] .

The Q-band represents absorption of light and consequently excitation of electrons from the highest occupied molecular orbital (HOMO), namely the  $a_{1u}(\pi)$ , to the lowest unoccupied molecular orbital (LUMO), namely the  $eg(\pi^*)$  *i.e.*

$a_{1u} \rightarrow eg$  [27-29]. Furthermore, the transition from  $a_{2u}$  to  $eg$  ( $a_{2u} \rightarrow eg$ ) results in the B-band formation[27-29] . Figs. 6- 8 show the electronic spectra (UV-Visible) of compounds  $(NO_2)_4PcCu(II)$ ,  $(NH_2)_4PcCu(II)$  and (TPPT) respectively. the of 3- nitro and 3- amino derivatives of phthalocyanine compounds deposited as thin film. It is quite obvious that both  $(NO_2)_4PcCu(II)$  and  $(NH_2)_4PcCu(II)$  spectra, Fig. 6 and 7 exhibit a general feature of phthalocyanine compounds and they are the two characteristic bands with the main absorption at 285 and 315 nm (soret band) and in the range 685 and 740 nm (Q-band) respectively. The reduction of nitro groups to amino groups also causes changes toward the red shifts, (+30 nm for B band) and (55 nm for Q band). This may be attributed to the addition

of electron donating groups ( $NH_2$ ) at the nonperipheral of the phthalocyanine ring result in are shift to the near IR region due to the presence of the pair of electrons of the amine group. Also the red shifted in Q-band may be due to decrease in energy between various  $\pi \rightarrow \pi^*$  transitions of the phthalocyanine ring and increasing in periphery of complexes . The same observations were found in B-bands of complexes . [29-31]

Grafting phthalocyanine amino derivatives with poly- (1, 4-phenylene terphthalamide) gives (TPPT), Fig. 8. The electronic spectrum of (TPPT), show a B- band at 330 nm and Q-band at 730 nm. Conversion of compound  $(NH_2)_4PcCu(II)$  to groups to(TPPT), causes changes toward the red shift, (+15 nm for B band) and blue shift (10 nm for Q band).

To investigate the effects of the TPPT on the organic solar cells (OSCs), the photovoltaic characteristics of OSCs with and without TPPT were measured and compared. Fig. 1a shows a schematic illustration of the fabricated OSCs consisting of a BHJ P3HT:PCBM composite active layer and the PEDOT:PSS with the PSS-coated TPPT. We investigated the effect of TPPT on the photovoltaic characteristics of the OSCs.

Thin films of ITO/PEDOT:PSS:TPPT /P3HT:PCBM/Al and ITO/PEDOT: PSS/ P3HT:PCBM/Al for UV-vis absorption studies were prepared on ITO coated glass substrate. UV-vis absorption spectrum was presented in Fig. 2(a,b). The net absorbance of the PEDOT:PSS layer with the incorporated TPPT was obtained as shown in Fig. 2(a). We Observed that ,No enhanced light absorption was exhibited for the PEDOT:PSS layer after coated by TPPT. And on the other hand , in Fig. 2(b) both films show characteristic peaks for P3HT in 500–600nm range and PCBM at about 330 nm. Obviously, the intensity of the UV-vis absorption peaks slightly increased with TPPT. The reason for this observation can be attributed to the increase in scattering of light due to the use of metallic TPPT which leads to enhancing the light absorption efficiency. The light scattering lengthened the optical path in the active layer, thereby trapping it inside [19,20,30–34]. Second reason for the enhancement of the total excitons created in the active layer is that the energy dissipation is proportional to the intensity of the electromagnetic field [35].

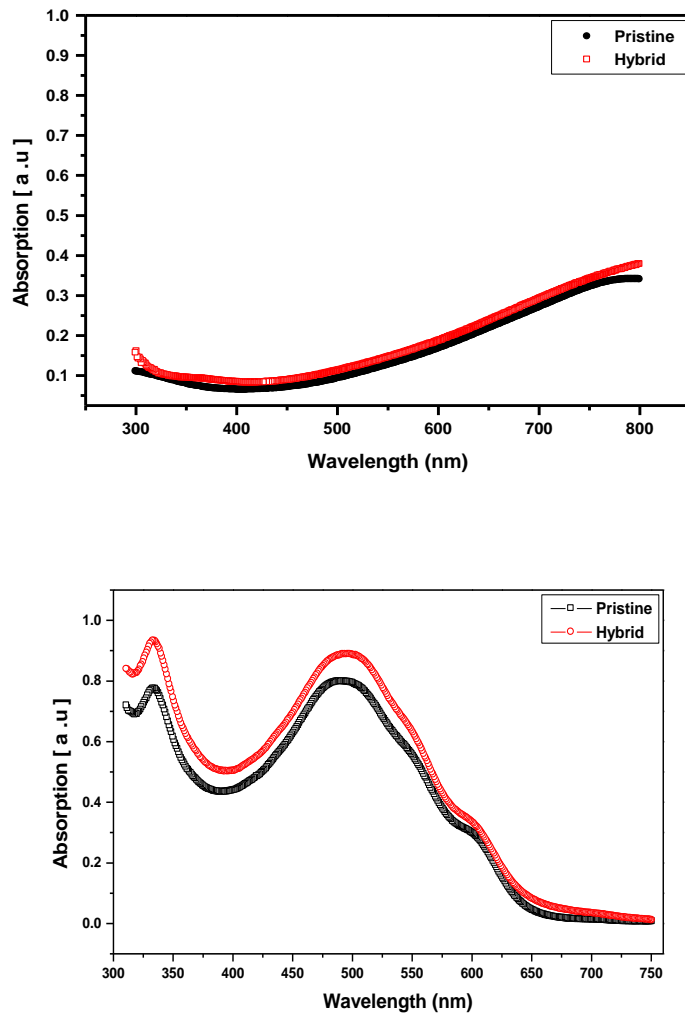


Fig.2. (a) UV-vis absorption spectra of pristine PEDOT:PSS layer and hybrid PEDOT:PSS:TPPT layer and (b) active layer/PEDOT:PSS layer and hybrid active layer/ PEDOT:PSS:TPPT layer thin films.

The current density (J) versus voltage (V) characteristics of devices were presented in Fig. 3. The device characteristics are summarized in Table 1. The open-circuit voltage ( $V_{oc}$ ) was increased from 0.54 to 0.6 V, whereas the short-circuit current density ( $J_{sc}$ ) and fill factor (FF) were increased from 0.3 to 0.38 mA/cm<sup>2</sup> and 0.046 to 0.089, respectively, for the hybrid photovoltaic cell when compared to the pristine photovoltaic cell. To obtain hybrid photovoltaic cells with higher current density and FF, both electron and hole mobilities must be optimized and most importantly, balanced. Hole is typically the high mobility carrier in regioregular P3HT and thermal annealing will further improve the hole mobility in the photovoltaic cell. The increased current density in hybrid photovoltaic cell compared to pristine photovoltaic cell may be due to the presence of inorganic throughout the active layer of P3HT: PCBM in hybrid film, which could increase the transport of charge-carriers in the hybrid photovoltaic cell. The incorporation of TPPT in PEDOT:PSS increases the interfacial contact area between the active layer (P3HT:PCBM) and PEDOT:PSS, allowing more efficient hole collection at the anode, and hence increases  $J_{sc}$  and FF. This increases the PCE of the hybrid photovoltaic cell up to 0.083% compared to pristine photovoltaic cell PCE of 0.14%.

To confirm the enhancement in the (PCE) of the OSCs, the EQE were measured. The IPCE for the reference and OSCs are shown in Fig. 6. We compared the curve of the increase in EQE between PEDOT:PSS and PEDOT:PSS: TPPT device. The photocurrent within the wavelength range from 400 to 700 nm increased significantly after addition of the TPPT. The EQE data supports the UV/visible data corresponding to Fig. 3. The device also showed enhanced quantum efficiency in the broad wavelength range due to adequate scattering of light. This indicates a shift in the improvement of optical absorption by the active layer near the PEDOT:PSS (with TPPT) buffer layer. We suggest that the enhanced of OSCs is mainly caused by the increase of optical absorption, because the incident light on the active layer could be intensified due to the surface plasmons of the TPPT at resonance frequency and/or the increase of the optical path of incident light by the scattering from TPPT. This is in good agreement with the trend of  $J_{sc}$ . The apparent discrepancy between light absorption and EQE can be explained by the fact that EQE measures the percentage of incident photons that eventually results in free charges being collected through the OSC electrodes. Factors beyond light absorption, such as the resistance of electrodes, exciton dissociation rate, and charge collection efficiencies will also affect the magnitude of PCE. However, such nonoptical effects are likely to be not wavelength sensitive and are represented by vertical shifts of the entire EQE spectrum. Comparing devices with or without TPPT in Fig. 4, it can be observed that the IPCE shows a wide band improvement from 400 to 650 nm. It therefore can be concluded that TPPT effects does not play a major role in improving PCE and electrical effects have to be accounted for.

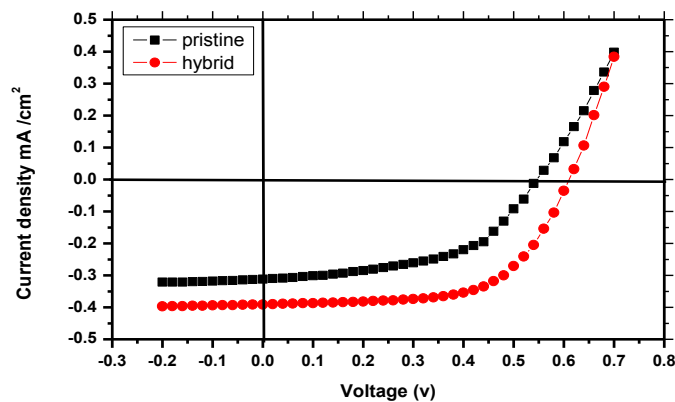


Fig.3 J-V curves of cells fabricated with pristine active layer/PEDOT:PSS layer and hybrid active layer/PEDOT:PSS:TPPT thin films.

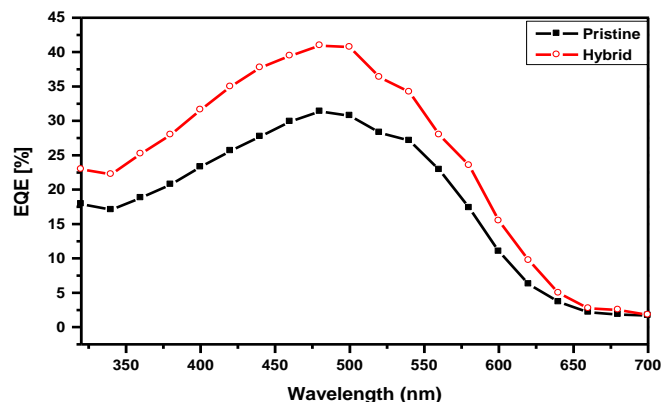


Fig.4. Incident photon-to-current conversion efficiency (IPCE) curves for the pristine and hybrid photovoltaic cells fabricated with PEDOT:PSS.

The bulk-heterojunction morphology of pristine PEDOT:PSS and hybrid PEDOT:PSS: TPPT films was investigated by atomic force microscopy (AFM). In order to understand the under laying morphology of the devices in the final photovoltaic cells, samples were made by removing the Al cathode from the final photovoltaic cells using sticky tape and the observed AFM images are showed in Fig. 4. The r.m.s roughness of the pristine PEDOT:PSS film is 6.9nm. The surface roughness increased to 9.2nm for the hybrid PEDOT:PSS: TPPT film. The increased roughness and the observed different texture of the hybrid thin film PEDOT:PSS: TPPT could be due to the presence of TPPT in the PEDOT:PSS layer which has undergone annealing process. The texture of the hybrid film PEDOT:PSS: TPPT is similar through out the surface of the film [36].

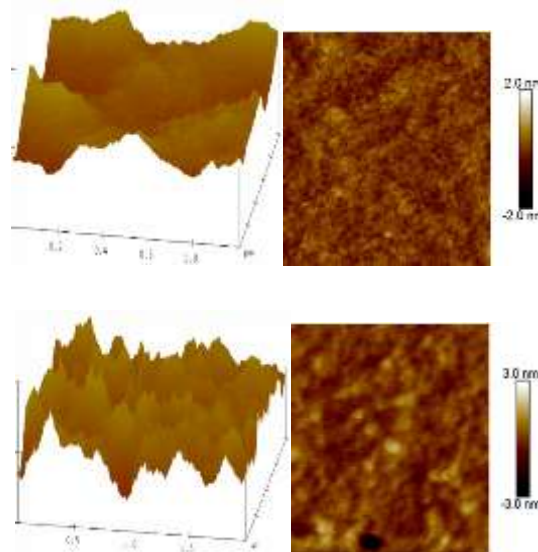


Fig.5. AFM images of the pristine PEDOT:PSS layer and hybrid PEDOT:PSS:TPPT layer thin films .

Table.1: Photovoltaic properties of the devices made with buffer layer and photoactive layer of P3HT to PCBM and TPPT.

Buffer layer	Voc(v)	Jsc(mA/ cm <sup>2</sup> )	FF	PCE (%)
PEDOT:PSS	0.54	0.30	0.046	0.083
PEDOT:PSS: TPPT	0.60	0.38	0.089	0.14

## V. Conclusion:

photovoltaic cells by generating the 3, 3', 3", 3'''-Tetra{ poly- (1, 4-phenylene terphthalamide)} phthalocyaninato copper (II) (TPPT)

in PEDOT:PSS light harvesting system for OSCs of P3HT:PCBM. Light absorption of device differs with TPPT and showed different Jsc due to much exciton generation. TPPT contributed in increased light harvesting. The presence of 3, 3', 3", 3' We fabricated the high efficient P3HT: PCBM hybrid "-Tetra{ poly-(1, 4-phenylene terphthalamide)} phthalocyaninato copper (II) (TPPT)

increased the charge-carrier mobility in the hybrid photovoltaic cell. We anticipate that this new concept of making hybrid polymer: fullerene: inorganic photovoltaic cells will be helpful to further improve the PCE of polymer photovoltaic in near future.

### Acknowledgment

The authors would like to acknowledge the Materials and Engineering Research Institute, Sheffield Hallam University, Sheffield S1 1WB, UK and University of Basra, College of Science, Department of Chemistry. The authors thank Dr. Aseel K. Hassan at Sheffield Hallam University for the opportunity to utilize his lab facilities and the solar simulator system for confirming our results

### REFERENCES

- [1] D. Wohrle and G. Meyer, "Phthalocyanine Properties and Application", VCH publishers, Cambridge (1996).
- [2] N. B. McKeown, "Phthalocyanine Materials: Synthesis, Structure and Function", Cambridge University Press (1998).
- [3] P. A. Barret, D. A. Frye, R. P. Linstead, *Chem. Soc.* , 1157(1938).
- [4] H. M. Frank, *Chem. Abs.*, **44**, 2567(1950).
- [5] W. M. Sander, *Chem. Abs.*, **61**, 12925(1958).
- [6] M. T. Sultan, Ph.D. Thesis, University of Baghdad, College of Education, 2007.
- [7] C.J. Brabec, N.S. Sariciftci and J.C. Hummelen, *Adv. Funct. Mater.*, **11**, 15(2001).
- [8] H. Spanggaard and F.C. Krebs, *Sol. Ener. Mater. Sol. Cells*, **83**, 125(2004).
- [9] K.M. Coakley and M.D. McGehee, *Chem. Mater.* **16** , 4533 (2004).
- [10] R.A.J. Janssen, J.C. Hummelen and N.S. Sariciftci, *MRS Bull.* ,**30** , (2005).
- [11] E. Bundgaard and F.C. Krebs, *Sol. Ener. Mater. Sol. Cells*, **91**, 954 (2007).
- [12] S. Gunes, H. Neugebauer and N.S. Sariciftci, *Chem. Rev.* ,**107**, 1324 (2007).
- [13] G. Yu, J. Gao, J.C. Hummelen, F. Wudl and A.J. Heeger, *Science*, **270**, 1789 (1995).
- [14] H. Hoppe and N.S. Sariciftci, *Mater. Chem.* , **16**, 45 (2006).
- [15] J.H. Hou, Z.A. Tan, Y. Yan, Y.J. He, C.H. Yang and Y.F. Li, *Am. Chem. Soc.* , **128**, 4911 (2006).
- [16] C. Shi, Y. Yao, Y. Yang and Q. Pei, *J. Am. Chem. Soc.* , **128**, 8980 (2006).
- [17] V. I. Vogel, Textbook of Practical Organic Chemistry, 4<sup>th</sup> Edition, Longman Scientific and Technology, UK, (1978).
- [18] B. N. Achar, G. M. Fohlen, J. A. Parker and J. Keshavaye, *Polyhedr.* , **6**, 1463(1987)
- [19] D. D. S. Fung, L. F. Qiao, W. C. H. Choy, C. Wang, W. E. I. Sha, F. X. Xie and S.L. He, **21**, 16348 (2011).
- [20] M. Jørgensen, K. Norrman and F. C. Krebs, *Sol. Ener. Mater. Sol. Cells*, **92**, 686 (2008).
- [21] J. P. Linsky and T. R. Paul, *Inorg. Chem.* , **19**, 331(1980).
- [22] M. P. Sama. J. Keshavaya and S. Sampath, *Pure Appl. Chem.* , 74(9), 1809(2002).
- [23] R. J. Palmer, Nylon and Polymers Plastic Encyclopedia of Polymers Science and Technology, 2001.
- [24] R. M. Silerstien, F. X. Webster and D. J. Kiemle, "Spectrometric Identification of Organic Chemistry Compounds ", 6th Ed. , John Wiley and Sons , N. Y, 2005.
- [25] R. I. Shriner and C. K. Hermann, " Spectroscopic Techniques for Organic Chemistry ", John Wiley and Sons , N. Y , 2004.
- [26] K. Nakamoto, "Infrared and Raman spectra of inorganic and coordination compounds " , J. Wiley and Sons LTD, USA , part B, 5th ed , 1997.
- [27] Mustafa H. Haider, M.Sc. Thesis, University of Basra, College of Science, 2014.

- [28] A. B. Lever, E.R. Milaeva, G. Speier, In Phthalocyanines: Properties and Applications, C. C. Leznoff, A. B. Lever (Eds.), VCH: Weinheim, Vol.3(1993).
- [29] A.B.Lever,"Inorganic Electronic Spectroscopy ", 2nd Ed., Elsevier science , 650 (1984).
- [30]F.C.Krebs,M.Jørgensen,K.Norrman,O.Hagemann, J. Alstrup,T.D.Nielsen,J.Fyenbo,K.L arsen and JetteKristensen, *Sol.Ener. Mater. Sol. Cells*, **93**, 422 (2009).
- [31]K. L.Kelly, E. Coronado, L. L. Zhao, G. C. Schatz , *Phys. Chem. B*,**107**, 668 (2003).
- [32] S. A. Maier and H A. Atwater, *J. Appl. Phys.* , **98**, 101 (2005).
- [33] B. P. Rand, P. Peumans and S. R. Forrest, *Appl. Phys.*, **96**, 7519 (2004) .
- [34] F. Monestier, *Solar Ener. Mater. Solar Cells*, 405 (2007).
- [35]E.K.Park, M. Choi, J.H. Jeun, K.T. Lim, J.M.Kim and Y.S. Kim, *Microelectr. Engin.* , **111**, 166 (2013).
- [36] H. Nguyen, H. Hopee, T. Erb, S. Gunes, G. Gobsch and N.S. Sariciftci, *Adv. Funct. Mater.*, **17**, 1071 (2007).

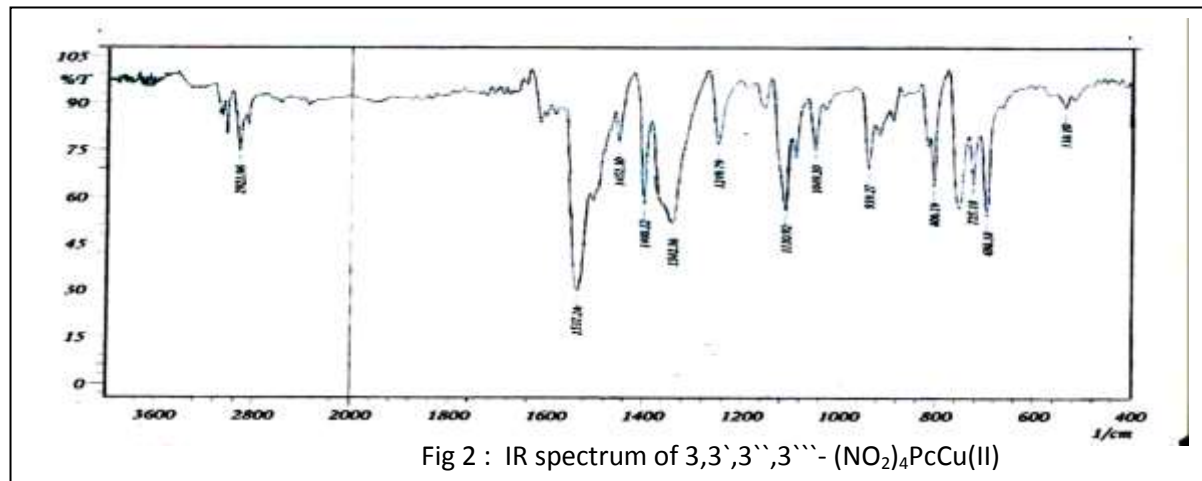


Fig 2 : IR spectrum of 3,3',3'',3'''-(NO<sub>2</sub>)<sub>4</sub>PcCu(II)

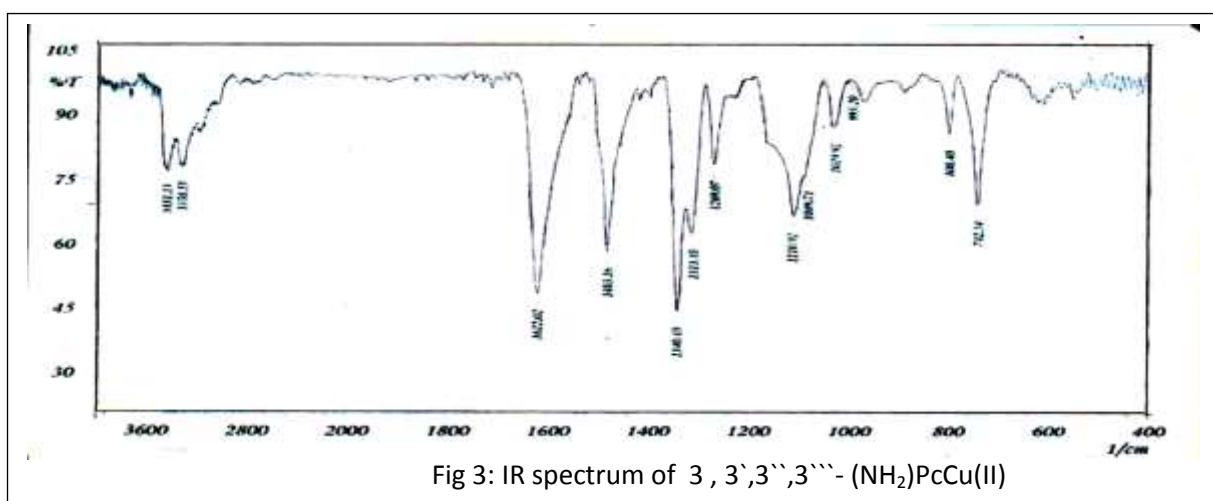


Fig 3: IR spectrum of 3,3',3'',3'''-(NH<sub>2</sub>)PcCu(II)

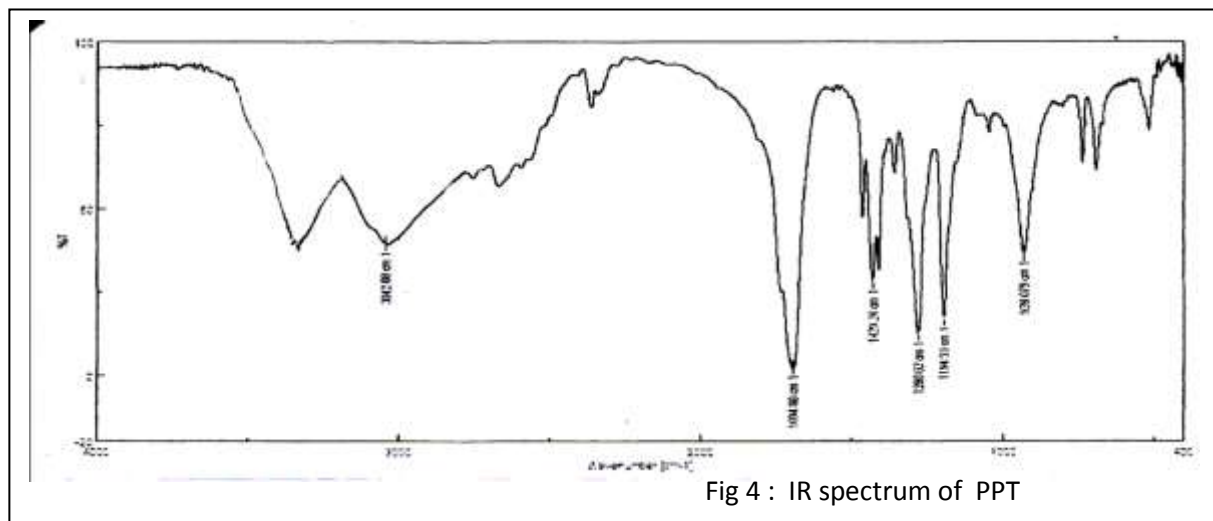


Fig 4 : IR spectrum of PPT

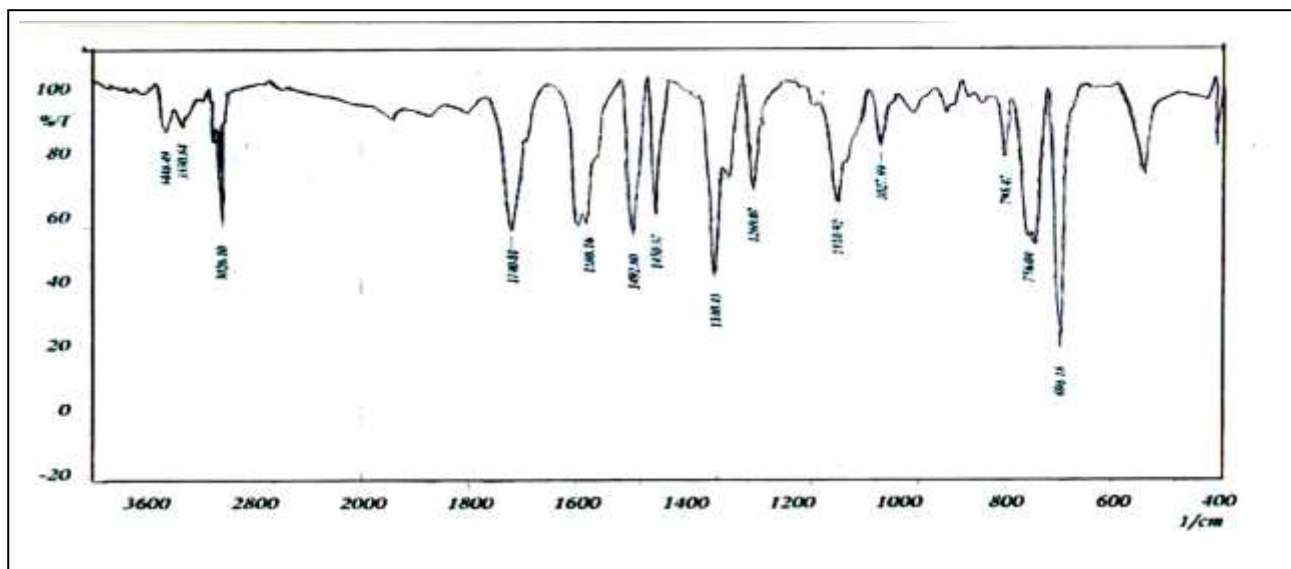


Fig 5 : IR spectrum of TPPT